15. SITE 746[1]

Shipboard Scientific Party[2]

HOLE 746A

Date occupied: 10 February 1988

Date departed: 12 February 1988

Time on hole: 2 days, 2 hr

Position: 59°32.82′S, 85°51.78′E

Bottom felt (rig floor; m; drill-pipe measurement): 4070.0

Distance between rig floor and sea level (m): 10.5

Water depth (drill-pipe measurement from sea level, m): 4059.5

Total depth (rig floor; m): 4350.8

Penetration (m): 280.8

Number of cores (including cores with no recovery): 16

Total length of cored section (m): 280.8

Total core recovered (m): 95.07

Core recovery (%): 33

Oldest sediment cored:
Depth sub-bottom (m): 280.8
Nature: diatomaceous silty clay
Earliest age: late Miocene
Measured velocity (km/s): 1.564

Principal results: Ocean Drilling Program (ODP) Site 746 (59°32.82′S, 85°51.78′E; water depth 4059.5 m) was offset about 5 km north of Site 745 and located over a seismically equivalent section so that the drilling program begun at Site 745 could be continued after a menacing iceberg had disrupted operations at that site. The section above 106.8 m below seafloor (mbsf) was washed at Site 746, a spot core was taken between 106.8 and 116.3 mbsf to establish correlation with Site 745, and continuous coring extended in one hole from 164.8 to 280.8 mbsf.

The lower Pliocene and upper Miocene mixed biogenic and terrigenous sediments recovered at this site consist of two lithologic units. Unit I can be divided into two subunits. Subunit IA is a locally bioturbated clayey diatom ooze, diatomaceous clay, and silty clay. Subunit IB is lithologically identical to Subunit IA except for its greater degree of lithification and more pervasive burrowing and bioturbation. Unit II is a locally developed nannofossil ooze with minor diatoms. Small clasts, interpreted as dropstones, are randomly dispersed throughout by ice rafting. The occurrence of well-sorted silty layers in part of the sequence is attributed to transport and sediment reworking by bottom currents. The biosiliceous sediment recovered at Site 746 is readily datable by diatoms and radiolarians, but calcareous microfossils are sparse and sporadic and of little use for biostratigraphy. The Miocene/Pliocene boundary occurs above 164.8 mbsf in the noncored interval, and uppermost Miocene sediment at the top of the continuously cored interval contains warmer water diatoms of the genera *Thalassiosira* and *Nitzschia*, as were found at Site 745. The same diatoms were also recorded in equivalent uppermost Miocene intervals on the southern (Sites 738 and 744) and the northern Kerguelen Plateau (Site 737). The oldest sediments cored at Site 746 (280.8 mbsf) are late Miocene in age.

BACKGROUND AND OBJECTIVES

Site 746 was occupied so that the drilling operation begun at nearby Site 745 could be continued after an iceberg at that latter site had disrupted operations there. Consequently, the objectives at Site 746 were the same as those at Site 745, namely to sample the sediment ridge off the southeastern flank of the southern Kerguelen Plateau in order to provide a deep-water Neogene reference section for paleoceanographic and sedimentological studies.

Site 746 is about 5 km north of Site 745 on the same sediment ridge, and, according to seismic stratigraphy, it should contain a very similar section to that of Site 745. Consequently, the top part of Site 746 was washed and continuous coring begun at a depth of 164.8 mbsf, the depth at which seismic stratigraphy and biostratigraphy predicted that an acceptable overlap of at least 20 m could be obtained between the sections cored at Sites 745 and 746. The next objective at Site 746 was to continue coring to as deep as possible until operations time expired.

SITE GEOPHYSICS

Site 746 was drilled about 5 km from Site 745 (Fig. 1). The new site was chosen because a menacing iceberg required operations to be terminated at Site 745. The ship moved between the

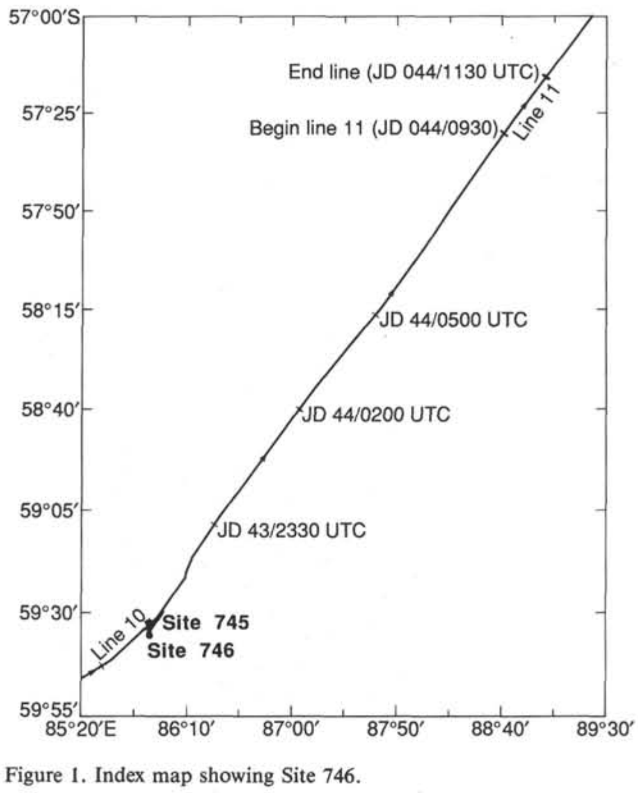

Figure 1. Index map showing Site 746.

[1] Barron, J., Larsen, B., et al., 1989. *Proc. ODP, Init. Repts.*, 119: College Station, TX (Ocean Drilling Program).

[2] Shipboard Scientific Party is as given in the list of Participants preceding the contents.

sites (ODP line 119-11) at 1 kt in calm seas with pipe hanging beneath the ship. The 3.5- and 12-kHz bathymetric systems were used to monitor water depths, but the seismic system was not deployed. The beacon for Site 746 was dropped near the point at 1000 hr along seismic line 119-10 (Fig. 2).

OPERATIONS

Site 746—Kerguelen Sediment Ridge

Hole 746A

An alternate drilling location was selected on the same local ridge of sediment as Site 745, near the reference seismic line and out of immediate danger from approaching icebergs. The move was made during the Global Positioning System (GPS) satellite window, so a round trip of the drill string was not necessary. The vessel was slowly offset on GPS to a position about 5 km to the north.

The objective of the site was to continue coring the stratigraphic section that had been started at Site 745. The hole was therefore drilled to 164.8 mbsf, with only a single core taken with the advance piston corer (APC) at 106.8–116.3 mbsf for a check of biostratigraphy. Continuous APC coring then began, but only one core could be recovered before still another iceberg forced an interruption. The iceberg passed just within the warning zone, and the delay was essentially a "short trip" to the seafloor for 2.5 hr.

APC coring then resumed, and a depth of 227.3 mbsf was reached before incomplete stroke and core liner failures indicated refusal depth (Table 1). Six extended core barrel (XCB) cores were taken to 280.8 mbsf when the familiar iceberg scenario was re-enacted. The newest intruder moved in from the northwest at about 1 kt and headed directly for the drill site. As

Table 1. Coring summary, Site 746.

Core no.	Date (Feb. 1988)	Time (local)	Depth (mbsf)	Length cored (m)	Length recovered (m)	Recovery (%)
119-746A-						
1W	11	0115	0–106.8	106.8	0.55	(wash core)
2H	11	0215	106.8–116.3	9.5	6.43	67.7
3W	11	0420	116.3–164.8	48.5	0.07	(wash core)
4H	11	0520	164.8–174.3	9.5	9.88	104.0
5H	11	0855	174.3–183.8	9.5	10.03	105.6
6H	11	0955	183.8–193.3	9.5	9.70	102.0
7H	11	1045	193.3–202.8	9.5	9.82	103.0
8H	11	1145	202.8–209.3	6.5	6.50	100.0
9H	11	1245	209.3–217.8	8.5	8.41	98.9
10H	11	1345	217.8–227.3	9.5	9.92	104.0
11X	11	1515	227.3–234.8	7.5	9.72	129.0
12X	11	1610	234.8–242.2	7.4	0.00	0.0
13X	11	1710	242.2–251.8	9.6	9.79	102.0
14X	11	1815	251.8–261.5	9.7	1.88	19.4
15X	11	1930	261.5–271.1	9.6	1.07	11.1
16X	11	2030	271.1–280.8	9.7	1.30	13.4
	(Coring)			125.5	94.45	75.3
	(Washing)			155.3	0.62	
				280.8	95.07	

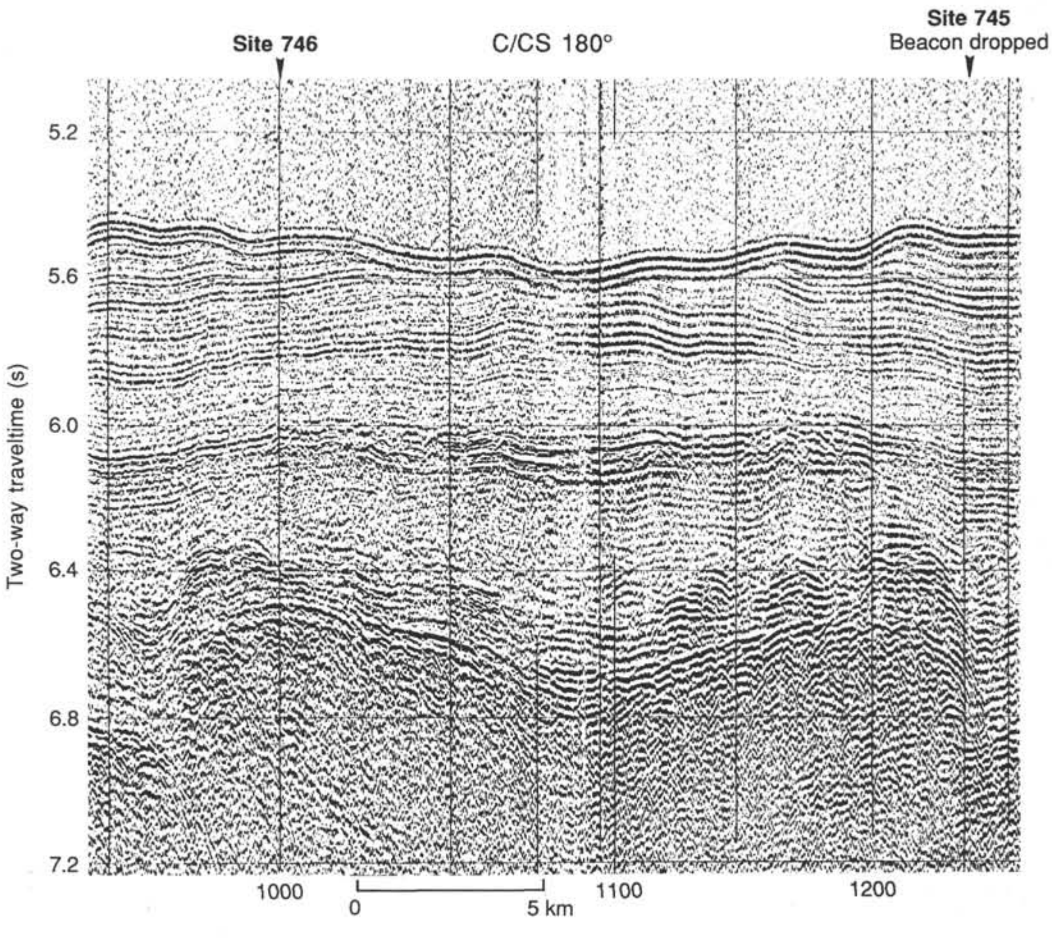

Figure 2. Vertical-incident seismic profile across Site 745 showing approximate location of Site 746.

too little time remained for either redrilling or reentering the hole after the iceberg moved on, drilling/coring operations were terminated for the voyage.

The early termination did present the opportunity to perform some bending stress tests on the drill string in relatively deep water. After the bit had been pulled clear of the seafloor and offset from the iceberg's path, the special strain-gauge-equipped drill-pipe joint was rigged and connected to the data recording unit and computer. The plan had been to simply turn the vessel into the "trough" and let the ship's roll provide the necessary deflections for the stress readings. However, the waves decreased to nearly nothing, and we spent an additional 2.5 hr pumping ballast to list the ship 5° to starboard. A successful set of readings was taken with a drill-string length of 4001 m (124,740 kg). Twenty-eight stands of pipe were pulled, and a second set of readings was taken at 3207 m (102,060 kg). As the next 28-stand increment was started, the upper drilling-line spooling-guide roller assembly became fouled with plastic coating strips that were peeling off the drilling line. With the departure deadline fast approaching, the ensuing 2.25 hr delay forced cancellation of the third scheduled bending stress test.

The final pipe trip of Leg 119 then continued, and all drill collars were laid down for the long transit as heavy snow fell on the rig. The vessel departed the drill site at 2218 hr, 12 February.

LITHOSTRATIGRAPHY AND SEDIMENTOLOGY

The main objective of drilling at Site 746 was to continue coring the upper Neogene sequence drilled at Site 745. Drilling at this site penetrated to a depth of 280.8 mbsf after washing down to 106.8 mbsf. The interval from 106.8 to 164.8 mbsf is highly disturbed (Sections 119-746A-2H-1 to 119-746A-2H-CC) and washed (Section 119-746A-3W-CC). Continuous coring at this site began with Core 119-746A-4H (164.8–174.3 mbsf). Core recovery was generally good (75%) except in the lower part of the hole (Cores 119-746A-11X to 119-746A-16X), where it declined to 46%. This reduced core recovery coincides with the change over from APC to XCB coring. The sediments at this site are relatively homogeneous and consist of two lithologic units, one of late Miocene to early Pliocene age and the other of late Miocene age. Unit I can be divided into two subunits (Fig. 3). Subunit IA is a firm clayey diatomaceous ooze, diatomaceous clay, and silty clay. Subunit IB is similar in lithology to Subunit IA except that the sediment is more consolidated and shows a greater degree of bioturbation, including the presence of *Planolites* and *Zoophycos* burrows. However, nowhere is the lithification of this subunit sufficiently advanced to warrant the term "stone." Unit II is much paler in color and consists of a nannofossil ooze with minor diatoms. Small clasts are dispersed throughout both units, which are structureless apart from the burrowing and bioturbation.

Visual smear slide estimates of the biogenic and mineral components, as well as the sand-silt-clay fractions, were made from at least one sample per core. The results are shown on the barrel sheets. Shipboard carbonate analyses were carried out on samples used for physical-properties tests and on selected parts of the core (see "Organic Geochemistry" section, this chapter). A few samples were also run on the Lab-Tech particle-size analyzer. These results are also included on the barrel sheets.

Drilling Disturbance

The wash Cores 119-746A-1W (0–106.8 mbsf) and 119-746A-3W (116.3–164.8 mbsf) bore loose, downhole material consisting of washed-out, ice-rafted clasts and lumps of clayey diatom ooze. Core 119-746A-2H (106.8–116.3 mbsf) was extremely liquid throughout, but was mostly intact and had a soupy disturbance only in the upper 45–60 cm. Through the hydraulically piston-cored intervals below 164.8 mbsf, bowed laminae were the principal expression of deformation, although soupy material (probably downhole contamination) was found in Cores 119-746A-4H, 119-746A-5H, 119-746A-7H, and 119-746A-13X. Piston core flow-in (suction) structures were noted in Sections 119-746A-10H-6 and 119-746A-10H-CC. Drilling fractures and biscuiting appeared in the comparatively stiff lithologies at and below Core 119-746A-8H, the top 43 cm of which consists of void and drilling breccia.

Lithology

Unit I

Sections 119-746A-2H-1 through 119-746A-2H-CC, 19 cm, and 119-746A-4H-1 through 119-746A-16X-CC, 30 cm, with the exception of 119-746A-13X-4 through 119-746A-13X-4, 58 cm; depth, 106.8–116.3 and 164.8–280.8 mbsf, except for 246.7–247.3 mbsf.
Age: late Miocene to early Pliocene.

Unit I consists of a relatively homogeneous, mixed biogenic and terrigenous sequence of sediments that form part of a more continuous sequence drilled at Site 745 (0–215 mbsf). Diatoms dominate the biogenic component and occur throughout the unit; however, they may be locally subordinate to nannofossils or clay. Smear slide examination of the nonclay fraction shows that quartz and feldspar are the most important nonbiogenic components, although they are always subordinate to diatoms. The unit can be divided into two subunits (Fig. 3). Subunit IA is a diatomaceous ooze with diatomaceous clay and silty clay. Subunit IB is lithologically similar to Subunit IA except that the sediment is more consolidated and more intensely burrowed and bioturbated.

The clay content increases with depth concomitant with an increase in the abundance of diatomaceous clay and silty clay. Color banding, believed to be of diagenetic origin, occurs throughout the unit. The bands show a close relationship with the more clay-rich parts of the sequence (Fig. 3).

Subunit IA

Sections 119-746A-2H-1 through 119-746A-2H-CC, 19 cm, and 119-746A-4H-1 through 119-746A-9H-CC, 25 cm; depth, 106.8–116.3 and 164.8–217.8 mbsf.
Age: late Miocene to early Pliocene.

Subunit IA consists of clayey diatomaceous ooze alternating with diatomaceous clay and silty clay. The amount of clay, silt, and diatoms varies considerably, even over short distances, with the result that lithologies are often complexly intermixed. The lithologies show a crude cyclic repetition (Fig. 3), with individual lithologies ranging from 6 to 73 cm in thickness. The uppermost part of this subunit (106.8–164.8 mbsf) is highly disturbed and soft (Sections 119-746-2H-1 to 119-746A-2H-CC).

The boundaries between lithologies are gradational or less commonly sharp; the main distinction between them is in the color and texture of the cut surface of the core. For example, diatomaceous clay and silty clay have a much smoother cut surface and are generally darker in color. The subunit shows a variety of colors, often intermixed, in various shades of green and gray; these include gray (5Y 5/1), grayish green (5G 5/2), and greenish gray (5GY 5/1 and 5GY 6/1). Parts of the subunit have a distinct reddish hue.

Coarse sand grains, granules, and minor small pebbles are uniformly disseminated throughout the subunit (gravel content <2%). Most clasts are fresh, subrounded to subangular, and composed predominantly of quartz. However, the larger pebble-size clasts show a wider range of lithologies and include granite, amphibolite, and various types of gneiss.

Darker gray, greenish gray, and bluish gray (5B 5/1) color bands occur at intervals throughout the subunit, individually or

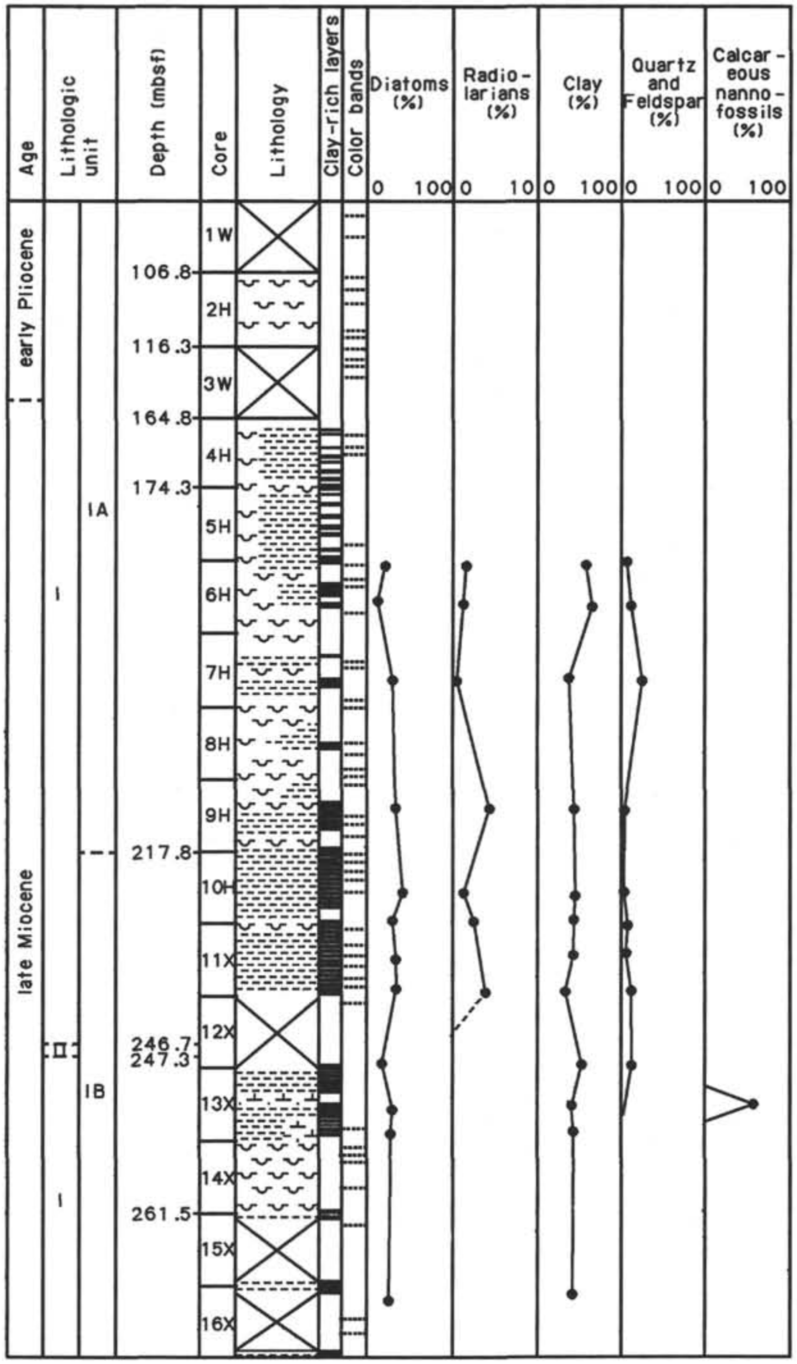

Figure 3. Lithologic summary at Site 746.

in closely spaced groups of up to five bands. Individually, the bands have diffuse or less commonly sharp boundaries, and they range from 2 to 15 mm in thickness. Spacing between bands likewise varies up to a maximum of 2.5 cm. The bands cut through other structures and appear to have a chemical diagenetic origin. Paler streaks and patches of silt <2 cm thick occur at intervals throughout the subunit but are not common. These generally have sharp bases and lack bioturbation, indicating that they were introduced fairly rapidly. Smear slide examination shows that they are remarkably well sorted, ungraded, and contain significant but minor amounts of diatoms, feldspar, and mafic minerals. All the minerals appear fresh and show no signs of abrasion.

The subunit is locally mottled and bioturbated. This becomes more common and less diffuse in the lower part of the subunit, probably in response to the increasing consolidation of the sediment. Evidence of this is also seen in the incipient fracturing of the cores at this stratigraphic level. Physical-properties studies show that all the sediments at this site are essentially underconsolidated (see "Physical Properties" section, this chapter).

Subunit IB

Sections 119-746A-10H-1 through 119-746A-16X-CC, 30 cm, with the exception of 119-746A-13X-4 through 119-746A-13X-4, 58 cm; depth, 217.8-280.8 mbsf, except for 246.7-247.3 mbsf.
Age: late Miocene.

Subunit IB is characterized by diatomaceous clay and silty clay alternating with clayey diatomaceous ooze. Lithologically, it is identical to Subunit IA. However, the two lithofacies can be distinguished on the basis of (1) increased consolidation of the sediment, (2) a greater proportion of clay (diatomaceous clay and silty clay dominate over diatomaceous ooze), (3) the presence of more abundant fractures and fracture zones, and (4) more pervasive bioturbation and burrowing. The boundary between these subunits is gradational and arbitrarily placed. The sediments are well consolidated, relatively homogeneous, and greenish gray (5G 5/1, 5BG 5/1, and 5GY 5/1) to gray (5Y 5/1) in color, with local reddish mottles and hues. They are weak to moderately bioturbated and burrowed. Both *Planolites* and *Zoophycos* burrows are fairly common, and in one example a *Planolites* burrow was displaced by a small fracture. The presence of these fractures and fracture zones in this subunit reflect the well-consolidated, more brittle nature of the sediments. Most of the burrows are horizontal to subhorizontal and may impart a crude "pseudolamination" to the sediment. The degree of burrowing and bioturbation is variable within the same section, with heavily bioturbated and burrowed zones adjacent to zones only weakly bioturbated (Fig. 4). Although the boundary between these zones is usually gradational, in some cases it is sharp and irregular. Coarse sand grains, granules, and small pebbles are disseminated throughout the subunit (Fig. 4), the majority of which appear to be *in situ*.

The crudely cyclic repetition of lithologies noted for Subunit IA is less obvious in this subunit because of the poor core recovery in the middle and lower parts of the sequence (Fig. 3). Diagenetic color banding is more common in this subunit (Fig. 4), with some displaced in a complex manner by microfractures (Fig. 5).

Unit II

Sections 119-746A-13X-4 through 119-746A-13X-4, 58 cm; depth, 246.7-247.3 mbsf.
Age: late Miocene.

Unit II consists of a 58-cm-thick, gray (5Y 5/1) to light gray (5Y 7/1), moderately well-consolidated nannofossil ooze containing up to 25% diatoms. Texturally, it is comprised of 3% sand, 86% silt, and 11% clay. Smear slide analysis shows that the only other components apart from nannofossils (65%) and diatoms (25%) are radiolarians (2%), clay (5%), and opaque minerals (2%). The boundary of this unit with Subunit IB is gradational. The lower boundary, for example, gradually becomes darker and passes into a greenish gray diatomaceous silty clay. The unit is moderately to intensely bioturbated throughout.

Interpretation

The sediments at Site 746 represent a mixed biogenic and terrigenous sequence, but with a dominance of biogenic components. The most abundant biogenic components are diatoms, which are mainly planktonic. Variations in diatom abundance, therefore, may reflect changes in surface-water productivity during glacial and interglacial stages or dissolution or both (Zimmerman et al., 1985). Sedimentation was fairly uniform and homogeneous. The very low, localized carbonate content indicates that the units were generally situated below the carbonate compensation depth (CCD).

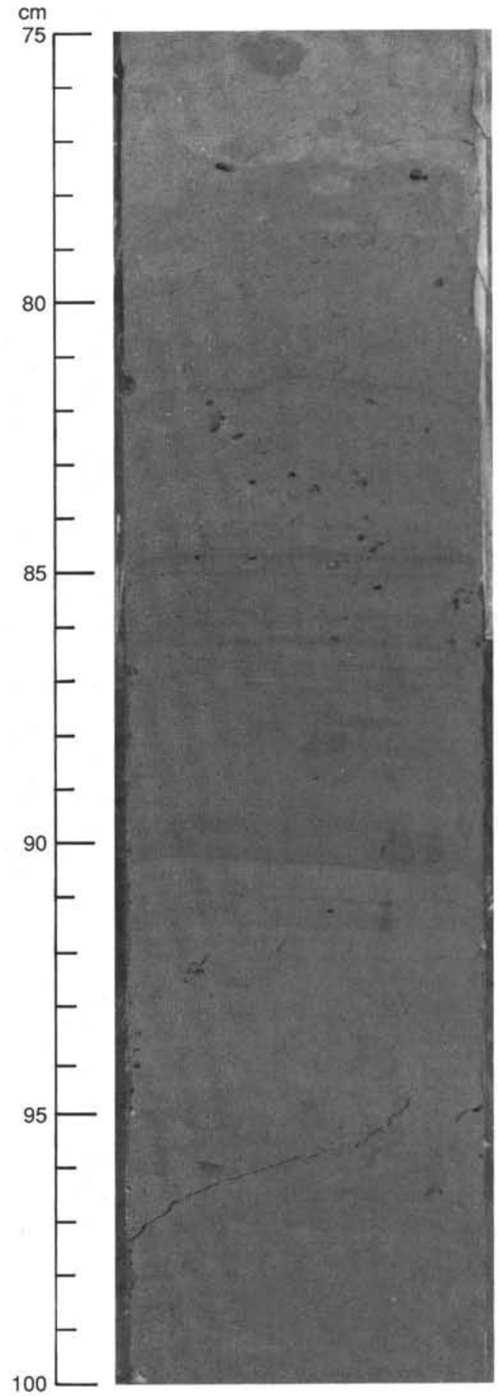

Figure 4. Sedimentary characteristics of Subunit IB: color banding, randomly scattered coarse sand grains and granules, and diffuse bioturbation (Section 119-746A-10H-5, 75–100 cm). Note the contact between the paler bioturbated zone (75–79 cm) and the darker, less well-burrowed zone below.

The structureless, poorly sorted nature of these fine-grained sediments is consistent with the emplacement of the silt and clay fraction by ice rafting. The randomly dispersed, coarse sand grains and gravel were probably dropped by icebergs floating over the site. The composition of some of the clasts clearly points to Antarctic basement as the source area, although a glacial input from Kerguelen Island cannot be ruled out.

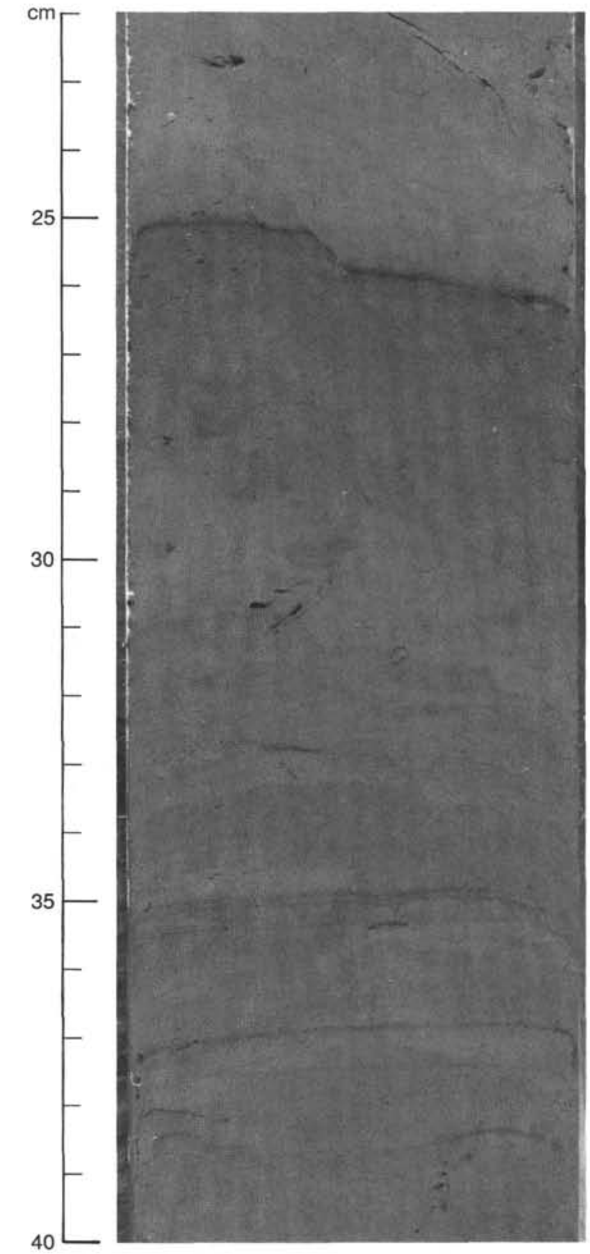

Figure 5. Microfractures displacing color bands and large *Planolites*-type burrow structures (Section 119-746A-10H-3, 22–40 cm). Note the *Zoophycos* burrow on the left (33.5 cm) and the "pseudolaminar" appearance of part of the core caused by the horizontal to subhorizontal disposition of the burrows.

A seismically defined depression occurs between Site 746 and the southern Kerguelen Plateau where it crosses our seismic line. Although this depression could have acted as a sediment trap, its continuation farther north and its existence in the Pliocene or Miocene are both uncertain. Thus, density flows carrying sediment off the Kerguelen Plateau, especially the more elevated northern portion, may have played a role in sediment transport.

The possibility of bottom current activity is indicated by the presence of well-sorted silty layers that may have originated from transport and reworking by strong bottom currents. Sediment deposited in this manner seldom shows the normal pattern of grading attributed to density flows (Srivastava, Arthur, et al., 1985). The lack of bioturbation and sharp base to the silty layers implies that they must have been deposited rapidly. If bottom currents were responsible, then rapid fluctuations in current strength are a prerequisite. Evidence in support of sediment reworking is the persistent presence of reworked diatoms and radiolarians of various ages. The sediment also contains some benthic diatoms that lived in the photic zone. The increased level of bioturbation and burrowing and the presence of well-defined *Planolites* and *Zoophycos* burrows in Subunit IB indicate a well-oxygenated bottom at this time. The darker-colored bands intersecting other structures are attributed to changes in pore-water chemistry and diagenesis beneath the sediment/water interface.

BIOSTRATIGRAPHY

Encroaching icebergs at Site 745 caused our decision to move about 5 km north, to wash down to the chronostratigraphic level attained at the previous location, and, thereafter, to continuously core for the remaining time available. One core (119-746A-2H) was taken at 106.8 mbsf to check progress, and, after washing down again, continuous coring began at 164.8 mbsf and was terminated at 280.8 mbsf. The recovered sediments range from late Miocene to early Pliocene in age and consist of siliceous oozes.

Calcareous nannofossils are absent from most of the succession. Those recovered are strongly etched as a result of deposition near the CCD and are of little biostratigraphic value. Foraminifers were not recorded at this site. Diverse, well-preserved diatom assemblages are present in all core-catcher samples. In addition, abundant and well-preserved radiolarians occur in the upper part of the sequence recovered, but become less common below Core 119-746A-10H. The distribution of these groups indicates that the Miocene/Pliocene boundary occurs in the uncored interval above 164.8 mbsf (Fig. 6).

Calcareous Nannofossils

All 16 core-catcher samples from the recovered siliceous ooze sequence at Site 746 were barren of calcareous nannofossils. The only nannofossiliferous sample from this site is Sample 119-746A-13X-4, 36 cm. It contains abundant, strongly etched *Reticulofenestra perplexa* and common *Coccolithus pelagicus*, which are of little age-diagnostic value.

Foraminifers

No foraminifers were observed in the core-catcher samples from this site.

Diatoms

Early Pliocene and late Miocene age diatoms are abundant to common and well preserved to moderately well preserved in all core-catcher samples collected from Site 746.

The core-catcher sample from Core 119-746A-2H (113.23 mbsf) contains a lower Pliocene assemblage equivalent to the uppermost part of the *Nitzschia reinholdii* Zone. It closely resembles the assemblage of Sample 119-745B-17H-CC (148.5 mbsf) in its relatively common occurrence of *Azpeitia nodulifer* and absence of *Thalassiosira nativa*. This suggests that stratigraphic horizons in Hole 746A may lie approximately 35 m above equivalent horizons in Hole 745B.

Continuous coring at Site 746 began with Core 119-746A-4H (164.8–174.3 mbsf) and continued through Core 119-746A-16X (271.1–280.8 mbsf), the last core taken. Sample 119-746A-4H-1, 60 cm, correlates with the upper Miocene part of the *N. reinholdii* Zone below the last occurrence of *Thalassiosira miocenica*. The Miocene/Pliocene boundary thus occurs in the unrecovered interval above 164.8 mbsf in Hole 746A as compared

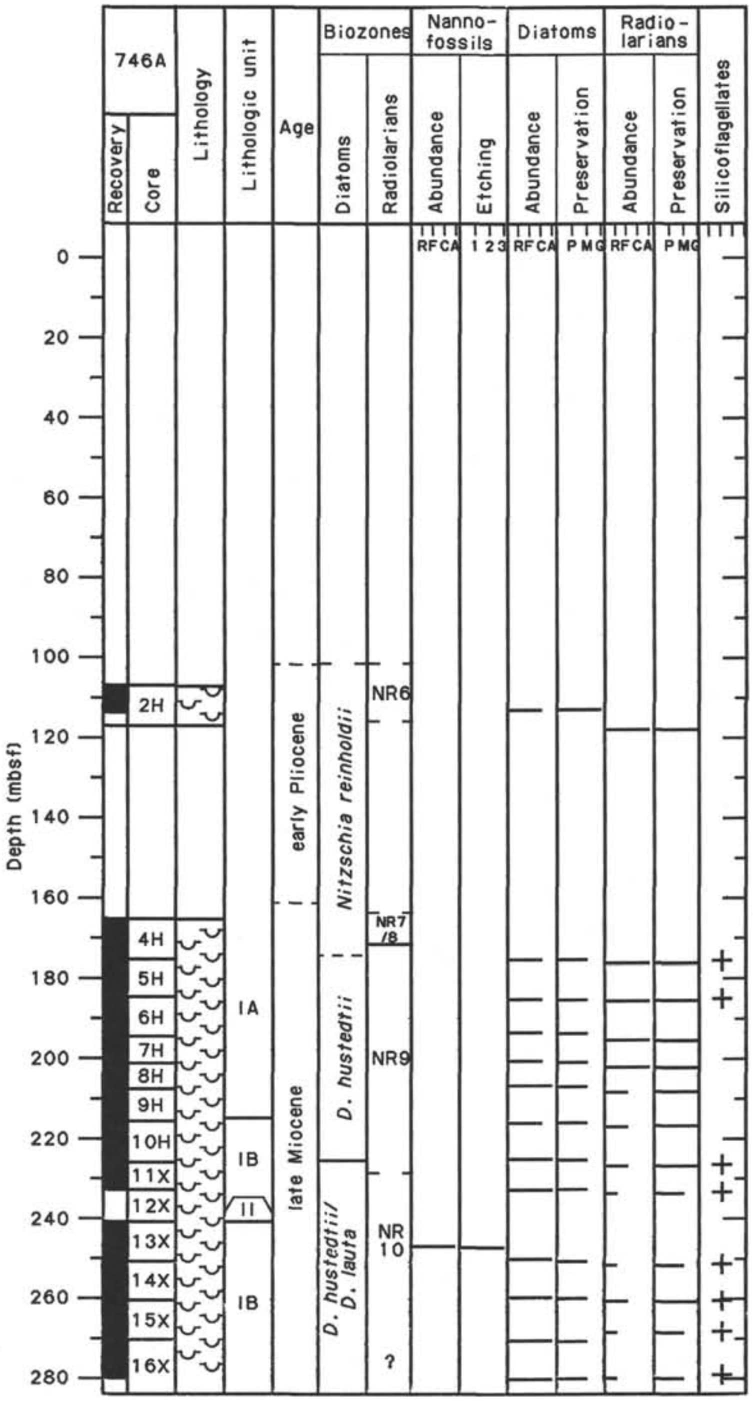

Figure 6. Biostratigraphic summary, Site 746.

with 206 mbsf in Hole 745B, indicating that stratigraphically equivalent horizons are at least 40 m deeper in Hole 745B than in Hole 746A.

Sample 119-746A-4H-4, 60 cm, is correlated with the *Denticulopsis hustedtii* Zone based on the common occurrence of the nominative species. The *D. hustedtii* Zone is characterized by common *D. hustedtii*, the presence of the distinctive acute triangular form of *Rhizosolenia hebetata*, and the lack of *Thalassiosira torokina* and *Denticulopsis dimorpha*.

Samples 119-746A-11X-CC through 119-746A-16X-CC are assigned to the upper part of the *Denticulopsis hustedtii/Denticulopsis lauta* Zone based on the consistent sparse to few occurrences of *D. dimorpha* and *D. hustedtii* var. *ovata* and the sporadic occurrence of *Denticulopsis punctata*. The results at ODP Site 689 (R. Gersonde, pers. comm., 1987) and studies at Site 744 suggest that *D. dimorpha* is only common in the lower portion (below 10 Ma) of the *D. hustedtii/D. lauta* Zone.

Radiolarians

Miocene to Pliocene radiolarian assemblages are abundant and well preserved in Cores 119-746A-2H through 119-746A-10X.

An Antarctic lower Pliocene assemblage was observed in Sample 119-746A-2H-CC. Species such as *Antarctissa ewingi, Desmospyris spongiosa, Pseudocubus vema*, and *Prunopyle titan* are diagnostic of the NR6 Zone. The occurrence of a rare specimen of *Helotholus*(?) *praevema*, which is the probable ancestor of *P. vema*, indicates a very early NR6 Zone. The low diversity of the radiolarian assemblage observed in Sample 119-746A-4H-CC does not allow us to place this sample in a very precise zone. The presence of *H.*(?) *praevema, P. titan*, and *Lychnocanium grande*, along with the absence of *Stichocorys peregrina*, indicates an early Pliocene–late Miocene age (NR7/8 Zones). The consistent occurrence of *S. peregrina* in a well-diversified assemblage places Sample 119-746A-5H-CC in the NR9 Zone. Many temperate forms, such as *Anthocyrtidium ophirense, A. ehrenbergi, Didymocyrtis antepenultimus*, and *Lamprocyclas hannai* gr., suggest a warmer interval at the end of the Miocene or the beginning of the Pliocene period. Samples 119-746A-5H-CC through 119-746A-10X-CC are related to the NR9 Zone. Below this interval, radiolarian assemblages are less abundant in diatomite oozes, and preservation fluctuates between good and moderate. Samples 119-746A-11X-CC through 119-746A-14X-CC fall within the NR10 Zone (middle Miocene to late Miocene). Abundant species are *Desmospyris haysi, Clathrocyclas bicornis spongothorax*, and *Stichopodium inflatum*. Sample 119-746A-15X-CC contains rare and moderately preserved radiolarians. No precise age can be assigned to this sample.

Palynomorphs

No palynomorphs were recorded from Site 746.

PALEOMAGNETICS

Hole 746A was APC cored to 227.3 mbsf and then XCB cored to 280.8 mbsf. Above 164.8 mbsf, Hole 746A was washed, except for the interval from 106.8 to 116.3 mbsf. The sedimentary sequence sampled consists of silty clay diatom ooze. From each 1.5-m section, two or three discrete samples were collected. We avoided sampling obviously disturbed intervals. The natural remanent magnetization (NRM) was measured on the archive halves of Cores 119-746A-1H to 119-746A-16X and for 123 discrete samples, using the shipboard cryogenic magnetometer. During the measurements of archive halves, all sections were demagnetized directly to 5 mT.

Figure 7 shows plots of NRM directions and intensities of the samples from Hole 746A. The NRM intensities varied between 0.2 and 25.0 mA/m. Many short-range fluctuations in NRM intensities present in this sedimentary sequence are similar to the results from Hole 745B. NRM determinations from archive halves are concordant with discrete sample determinations.

In Figure 8, NRM inclinations are plotted against depth downhole. Magnetic measurements show many clear normal reversal regions; however, correlation of these data with the standard reversal sequence (Berggren et al., 1985) is difficult. The NRM inclinations and intensities in Holes 745B and 746A are compared in Figure 9. Data from both holes between 160 and 180 mbsf show similar fluctuations in magnetic intensity and inclination. If this correlation is correct, this region is assigned to the Gilbert Chron. Referring to biostratigraphic data, the sequence under about 240 mbsf may be correlated to Chron C5. Shorebased demagnetization studies will be necessary to define the sequence in detail.

SEDIMENTATION RATES

On the basis of the diatom and radiolarian occurrences, the upper part of Site 746 (106.8 mbsf down to about 160 mbsf) is early Pliocene in age. The remaining section down to 280.8 mbsf is upper Miocene.

INORGANIC GEOCHEMISTRY

Site 746 is about 5 km north of Site 745 on the southeastern slope of the southern Kerguelen Plateau. Four whole-round minicores 5 cm in length were obtained from 171 to 248 mbsf for the purpose of interstitial-water chemical studies. The samples consist of upper Miocene clayey diatom ooze, diatomaceous clay, and silty clay (see "Lithostratigraphy and Sedimentology" section, this chapter) and contain 0.1%–4.6% calcium carbonate and 0.1%–0.2% organic carbon (see "Organic Geochemistry" section). Only two of the interstitial-water samples were taken from depths greater than the deepest sample obtained at Site 745. Therefore, the data from Site 746 do not significantly extend the information gained at Site 745, but can be used to verify chemical trends identified at the latter site.

Results

Site 746 interstitial-water samples were analyzed for pH, alkalinity, salinity, chloride, sulfate, magnesium, calcium, phosphate, ammonium, and silica using the methods outlined in the "Explanatory Notes" chapter (this volume). Charge-balance calculations were performed on each of the interstitial-water samples to check for gross irregularities in the data. Sodium and potassium were calculated by multiplying the ratio of each cation to chloride for average seawater, using the values given by Stumm and Morgan (1981), by the chloride concentration of each sample. All of the samples have charge imbalances $<2\%$, indicating that drilling contamination is minimal. All of the data obtained at Site 746 are displayed in Table 2.

Salinity and Chloride

Salinity and chloride analyses of the interstitial-water samples from Site 746 indicate that they are compositionally similar to the deepest samples from Site 745. The mean salinity of the Site 746 samples is 35.5 g/kg (s.d. = 0.2 g/kg, n = 4) vs. 35.7 g/kg (s.d. = 0.3 g/kg, n = 10) for the Site 745 samples. The mean chloride concentration from 171 to 195 mbsf at Site 746 is 559 vs. 556 mmol/L at 192 mbsf at Site 745. The differences in salinity and chloride concentration between depth-equivalent samples from Sites 745 and 746 are within the analytical precision of the data, adding validity to the assumption that the Site 746 samples can be used to extend the data from Site 745 to deeper levels.

Magnesium and Calcium

The linear correlation between dissolved magnesium and calcium observed at Site 745 also exists at Site 746 ($r = -0.948$). Dissolved magnesium concentrations decrease and dissolved calcium concentrations increase with increasing depth from 171 to 248 mbsf. The slope of the regression line describing the correlation between calcium and magnesium for the Site 746 samples is $-0.40°$ vs. $-0.48°$ for the Site 745 samples. These data indicate that magnesium and calcium also behave conservatively between 171 and 248 mbsf at Site 746 and that the diffusion properties of the sediments at both sites are quite similar.

Silica

Dissolved silica concentrations at Site 746 are quite variable between 171 and 248 mbsf (mean = 991 μmol/L, s.d. = 54 μmol/L, n = 4), but are similar in magnitude to the concentrations of the deepest sample at Site 745 (1010 μmol/L at 192 mbsf). Dissolution of biogenic silica continues to supply silica to the interstitial waters below 200 mbsf, and no reactions involving dissolved silica are apparent to a depth of 248 mbsf.

Alkalinity, Sulfate, Ammonium, and Phosphate

Sulfate analyses at Site 746 indicate that microbial catabolism occurs to at least a depth of 248 mbsf. Sulfate concentrations decrease from 21.2 mmol/L at 171 mbsf to 17.2 mmol/L at 248 mbsf. Dissolved ammonium concentrations do not continue to increase below 171 mbsf at Site 746, as appeared possi-

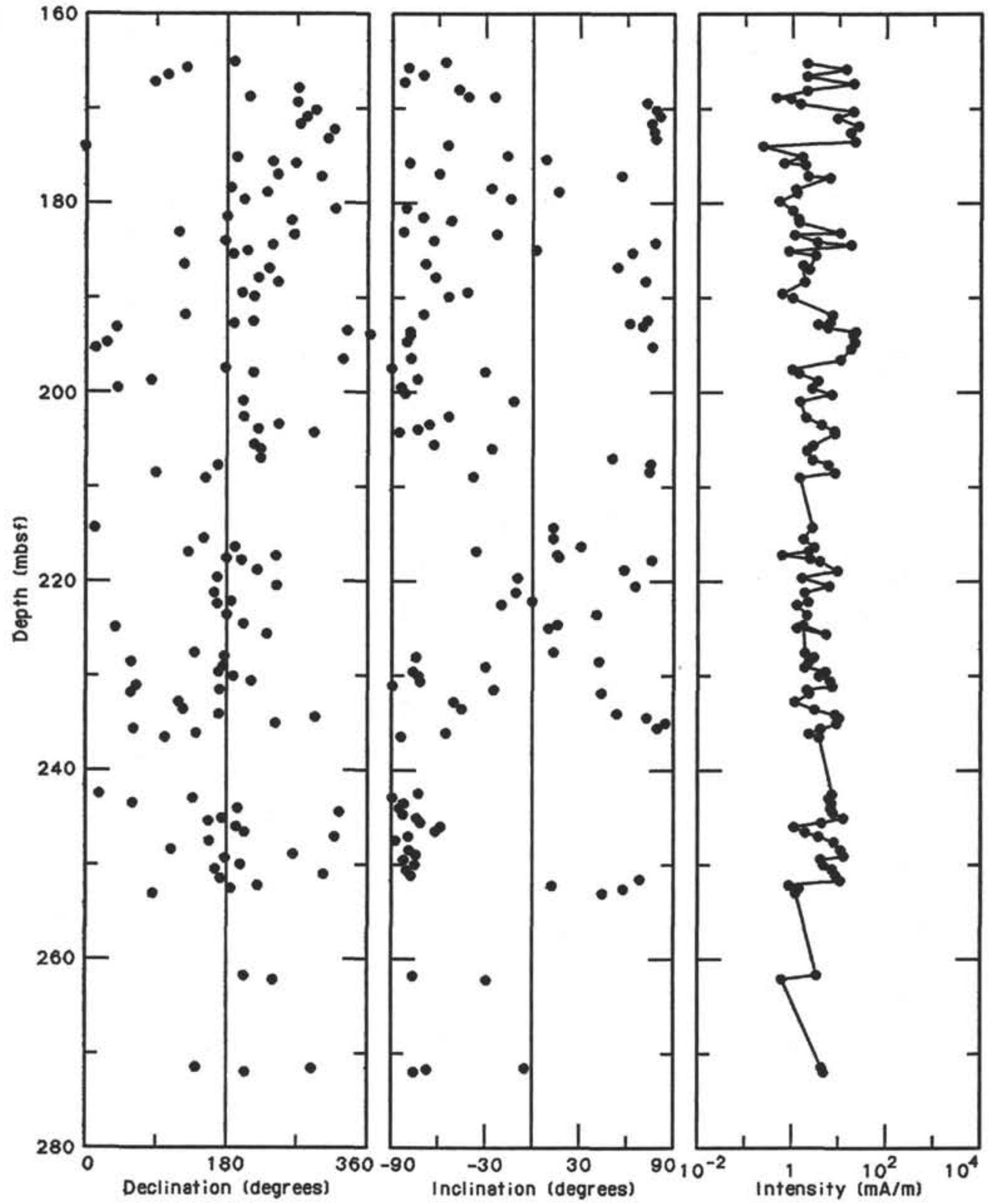

Figure 7. Plots of NRM declination, inclination, and intensity vs. depth, Hole 746A.

ble at Site 745. Phosphate concentrations are extremely low (2 μmol/L or less) below 171 mbsf. Bacterial sulfate reduction clearly is taking place at depths greater than 248 mbsf, but the low ammonium and phosphate concentrations indicate that the amount of organic matter being consumed at this depth is small. Alkalinity values between 171 and 248 mbsf are around 2 mmol/L lower than at 192 mbsf at Site 745. This implies that the amount of reactable organic matter originally present in the samples from Site 746 may have been lower than in stratigraphically equivalent sediments at Site 745.

ORGANIC GEOCHEMISTRY

Hole 746A was washed to 106.8 mbsf, cored from 106.8 to 116.3 mbsf, washed again to 164.8 mbsf, and cored to 280.8 mbsf. Organic geochemistry was studied on interstitial-water squeeze-cake, carbonate, and physical-properties samples, as outlined in the "Explanatory Notes" chapter.

Hydrocarbon Gases

The headspace procedure was used approximately every 30 m to determine hydrocarbon gases. All of the samples had <11 ppm methane. No ethane was detected at Site 746.

Carbon Analysis

Inorganic carbon was measured on the interstitial-water squeeze-cake, carbonate, and physical-properties samples (Table 3 and Fig. 10).

Carbonate content was <1% except for Sample 119-746A-13X-4, 145–150 cm, which had 4.6% carbonate. Organic carbon remained relatively constant from 0.09% to 0.16%. This is approximately the same as the level from Site 745 at 100 mbsf.

PHYSICAL PROPERTIES

The main objective of drilling at Site 746 was to continue coring the upper Neogene sequence drilled at Site 745, approxi-

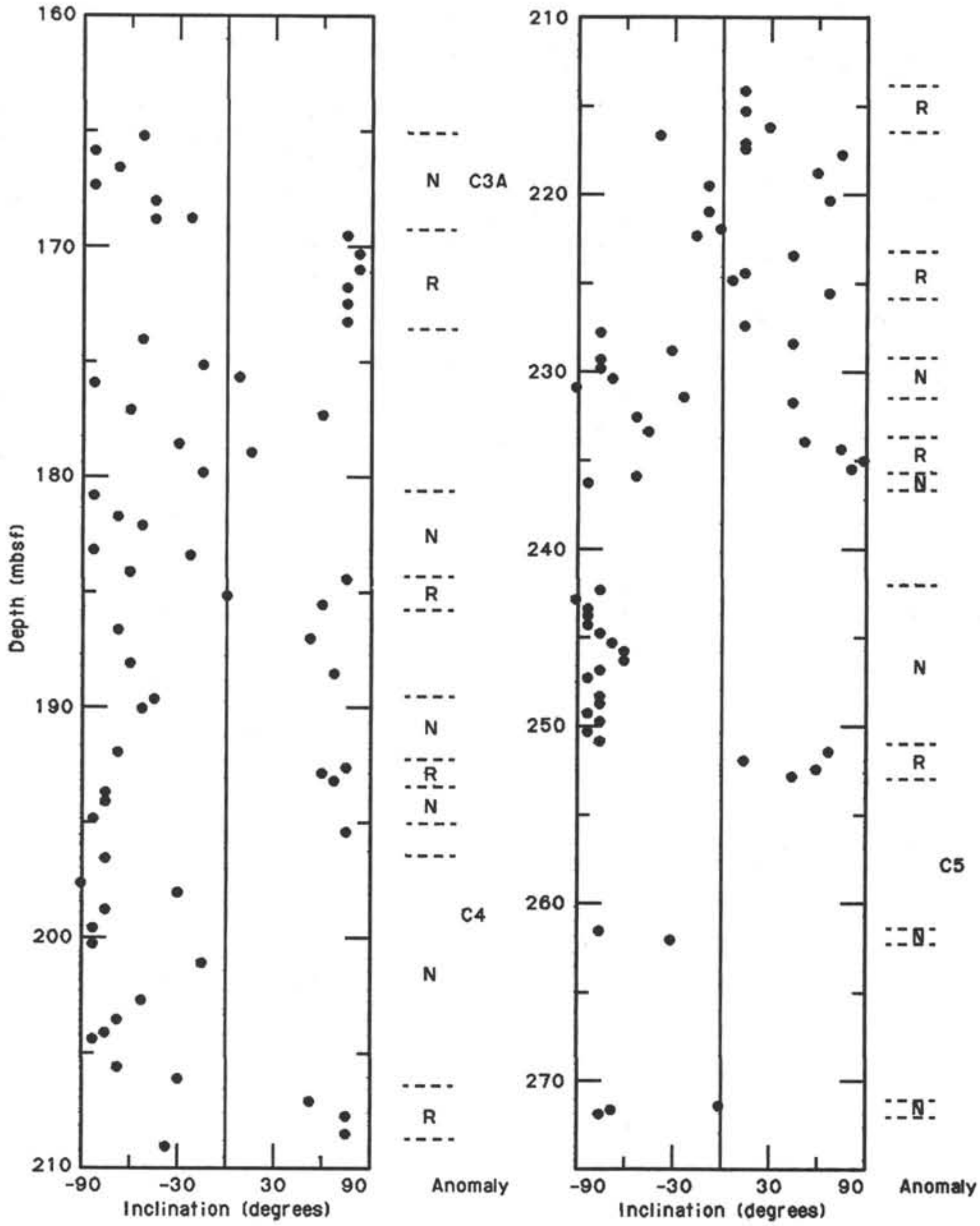

Figure 8. Plots of NRM inclination vs. depth, Hole 746A.

mately 5 km to the south, which had to be evacuated because of icebergs. Hence, the objectives of the physical-properties program were, as for Site 745, to contribute to the understanding of syndepositional and post-depositional processes in sediments on the Kerguelen Plateau and adjacent deep-sea areas. In particular, we hoped to establish the presence and nature of hiatuses and lithologic boundaries, which could have implications for glacial-interglacial fluctuations.

Physical properties measured were (1) index properties (water content, porosity, wet- and dry-bulk density, and grain density), (2) undrained shear strength, (3) compressional-wave velocity, and (4) thermal conductivity. Techniques and laboratory methods used are discussed in the "Explanatory Notes" chapter.

One hole, 746A, was drilled at this site, with continuous APC from 164.8 to 227.3 mbsf, and the XCB from 227.3 mbsf to total depth at 280.8 mbsf. Full core recovery was achieved in the upper half of the hole, but went down in the lower half, averaging 75.3% for the hole (see "Operations" section, this chapter). Core disturbance was relatively significant, mainly consisting of vertical flowage in the APC-cored part and biscuiting in the XCB-cored lower part. All physical-properties data are presented in Table 4 and Figure 11.

Results

Physical-properties profiles at Site 746 do not exhibit any significant changes that would justify a division into different geotechnical units. The index properties decrease with the same slight gradient defined at Site 745. Water content and porosity decrease approximately from 55% to 50% and from 75% to 70%, respectively, while bulk density increases from values of about 1.50 g/cm^3 to values around 1.55 g/cm^3. These parameters show a relatively small scatter, usually deviating <5% off a

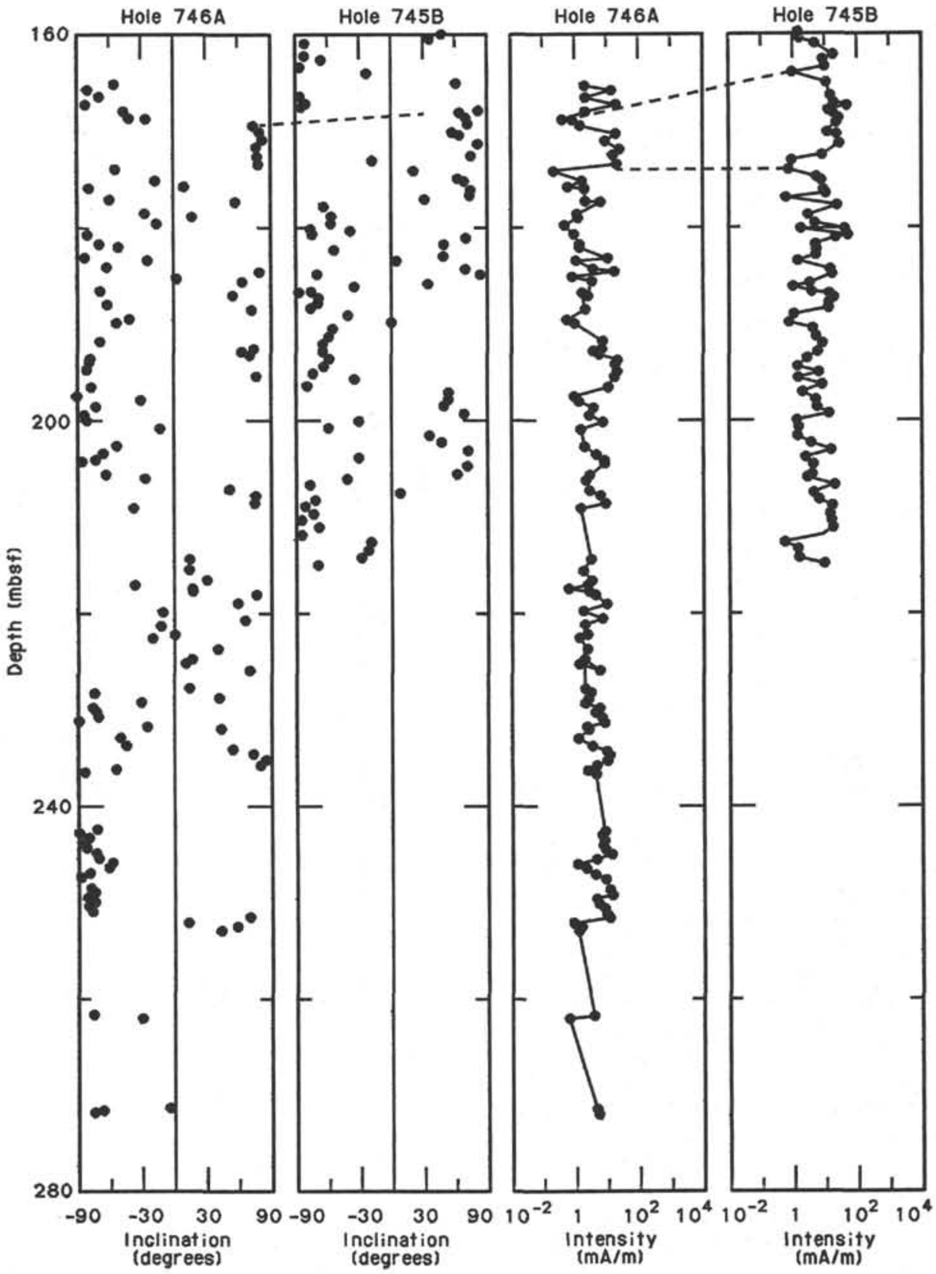

Figure 9. NRM inclination and intensity of Holes 746A and 745B vs. depth below 160 mbsf.

Table 2. Interstitial-water geochemical data, Hole 746A.

Core, section, interval (cm)	Depth (mbsf)	Volume (mL)	pH	Alkalinity (mmol/L)	Salinity (g)	Magnesium (mmol/L)	Calcium (mmol/L)	Chloride (mmol/L)	Sulfate (mmol/L)	Phosphate (μmol/L)	Ammonium (mmol/L)	Silica (μmol/L)	Mg^{2+}/Ca^{2+}
4H-4, 145-150	170.75	62	7.4	4.86	35.2	37.3	19.9	559	21.2	2	0.50	948	1.9
7H-1, 145-150	194.75	50	7.5	4.71	35.5	35.2	20.4	559	19.8	2	0.38	1017	1.7
10H-4, 145-150	223.75	45	7.3	4.66	35.8	34.0	21.5	562	17.4	1	0.43	944	1.6
13X-4, 145-150	248.15	45	7.2	4.33	35.5	32.6	21.6	561	17.2	1	0.45	1054	1.5

linear average. Grain density stays relatively constant, with an average of 2.55 g/cm^3, but shows a larger scatter, probably due to variations in the content of biogenic silica (i.e., diatoms).

The average shear strength measured with the fall cone increases with depth, although the gradient may be slightly smaller than in the lower unit of Site 745. As also observed at the previous Leg 119 sites, the fall cone shear strengths are higher than those measured with the vane shear. At this site, the vane shear strength averages 73 kPa, while the fall cone shear strength averages 122 kPa. Vane shear strengths, however, show a constant or possibly a slightly decreasing trend with depth at Site 746. Likely causes for a decrease or reversal of the depth gradient are variations in sediment composition and core disturbance. No significant compositional change has been recorded, but more

Table 3. Total carbon, inorganic carbon, organic carbon, and carbonate carbon data, Hole 746A.

Core, section, interval (cm)	Depth (mbsf)	Total carbon (%)	Inorganic carbon (%)	Organic carbon (%)	$CaCO_3$ (%)
2H-CC, 0–1	113.01		0.01		0.1
4H-4, 145–150	170.75	0.12	0.01	0.11	0.1
4H-6, 70–71	173.00		0.01		0.1
4H-CC, 0–1	174.40		0.02		0.2
5H-4, 90–92	179.70		0.09		0.8
5H-CC, 0–1	184.06		0.01		0.1
6H-2, 114–115	186.44		0.01		0.1
6H-CC, 0–1	193.32		0.01		0.1
7H-1, 145–150	194.75	0.10	0.01	0.09	0.1
7H-6, 94–95	201.74		0.08		0.7
7H-CC, 0–1	202.84		0.01		0.1
8H-4, 5–6	207.35		0.01		0.1
8H-CC, 0–1	208.90		0.03		0.3
9H-3, 96–97	213.26		0.01		0.1
9H-CC, 0–1	217.42		0.01		0.1
10H-4, 145–150	223.75	0.17	0.01	0.16	0.1
10H-6, 74–75	226.04		0.01		0.1
10H-CC, 0–1	227.24		0.02		0.2
11X-CC, 0–1	236.65		0.01		0.1
13X-4, 145–150	248.15	0.67	0.55	0.12	4.6
13X-CC, 0–1	251.70		0.01		0.1
14X-CC, 0–1	253.39		0.02		0.2
15X-CC, 0–1	262.21		0.01		0.1
16X-CC, 0–1	272.06		0.01		0.1

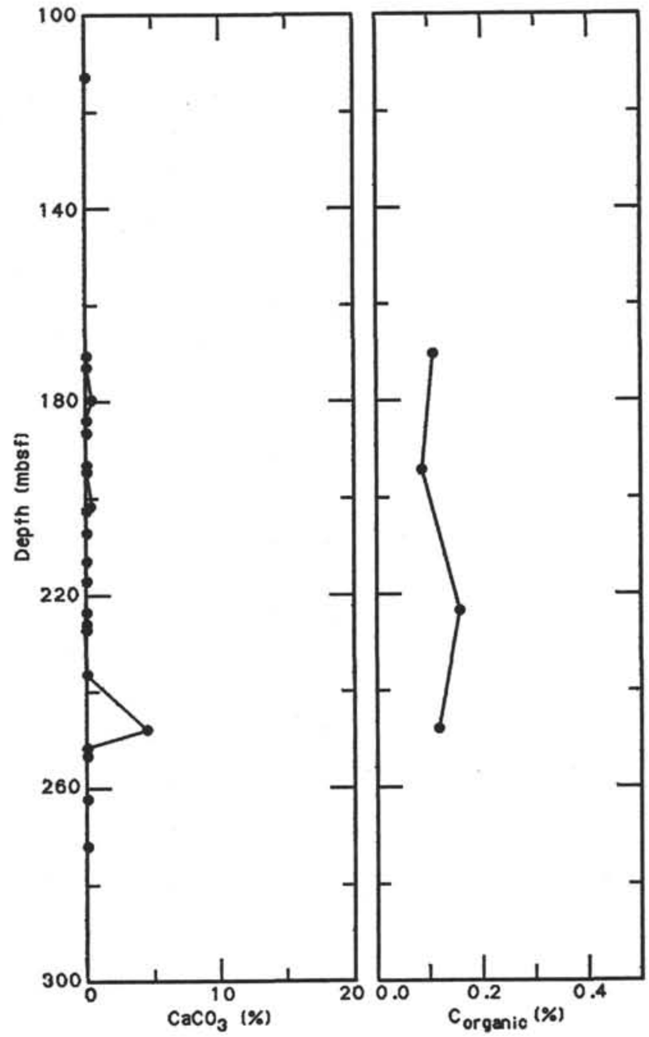

Figure 10. Carbonate carbon and organic carbon, Hole 746A.

detailed studies may reveal changes. Core disturbance may have increased with the onset of XCB coring at 227.3 mbsf. The reason for the difference between the two methods is probably a function of the different measuring techniques and their different response to variations in sediment composition and disturbance (see "Explanatory Notes" chapter).

Both measurements of shear strength show considerable scatter, with the largest in the fall cone values. The fact that the scatter in the two methods of measurement generally corresponds shows that it is not caused by measurement errors, but rather results from a combination of core disturbance and variations in composition. The clay-rich layers may tend to have higher values than the oozes, but this is not obvious. Variations could be caused by the different sediment types having different susceptibilities to core disturbance. As the fall cone study involves a smaller sample volume than the vane shear study, disturbed zones are more easily avoided with the fall cone method, although this again seems to be more affected by small-scale grain-size variations. This may be a reason for the apparent phase shift between the two methods in the large maximum-minimum cycle observed at about 225 mbsf, where severe disturbance appeared to occur.

Compressional-wave velocity is essentially constant, averaging 1560 m/s, throughout the cored sequence. The scatter is small—standard deviation is 21.5 m/s—reflecting the overall homogeneous nature of the cored sediments. Within the low values measured in these sediments, core disturbance does not seem to affect velocity.

Thermal conductivity was measured in up to four sections per core, depending on core recovery. The values show no significant trend, but are essentially constant, averaging 0.97 W/m/°C, thereby continuing the trend observed at Site 745.

Summary

The sedimentary sequence cored at Site 746 essentially shows a continuation of the trends found in the lower part of the drilled sequence at Site 745 and hence is considered to belong to geotechnical subunit G2C (see "Physical Properties" section, "Site 745" chapter, this volume). Water content and porosity follow a slight linear decrease with depth, and bulk density has a slight increase. Shear strength, despite a relatively large scatter, seems to become more constant with depth, relative to Site 745 trends, while compressional-wave velocity and thermal conductivity stay essentially constant. No major hiatuses apparently occur in the cored sequence, and this is confirmed by the physical-properties profiles, showing no signs of significant erosional events.

SEISMIC STRATIGRAPHY

The general geologic setting at Site 746 is described for Site 745 (see "Seismic Stratigraphy" section, "Site 745" chapter). Only the seismic correlation between the two sites will be dealt with here. A 3.5-kHz precision depth recorder (PDR) line was measured while the ship slowly moved from Sites 745 to 746. This line is the only direct seismic connection between the sites. Only seismic reflections from the upper 110 m were observed on this PDR record. Two reflectors were traced from Sites 745 to 746, and, assuming a sound velocity as in seawater (1485 m/s), correlation was established (see Table 5).

A single-channel seismic line was recorded approaching Site 745, with the trackline shown on Figure 1 in the "Site Geophysics" section (this chapter). This line crosses Site 745, but passes Site 746 about 1 km to the southeast, so a direct seismic correlation for the deeper reflectors is not possible; however, the correlations from Site 745 to the point nearest to Site 746 are shown for comparison in Table 5.

Table 4. Physical properties measured for Hole 746A.

Core, section, interval (cm)	Depth (mbsf)	Water content (%)	Porosity (%)	Bulk density (g/cm^3)	Dry-bulk density (g/cm^3)	Grain density (g/cm^3)	Undrained shear strength vane (kPa)	Undrained shear strength fall cone (kPa)	Compressional-wave velocity (m/s)	Thermal conductivity (W/m/°C)	Temperature drift rate (°C/min)	Curve-fitting parameter
4H-1, 82	165.62							86.0				
4H-2, 80	167.10						74.2					
4H-2, 81	167.11	54.88	75.33	1.46	0.66	2.53						
4H-2, 83	167.13								1543.3			
4H-4, 69	169.99						87.0					
4H-4, 70	170.00	52.44	73.30	1.49	0.71	2.51						
4H-4, 72	170.02							93.0				
4H-4, 73	170.03								1546.6			
4H-6, 70	173.00	53.89	74.58	1.50	0.69	2.53	95.1					
4H-6, 73	173.03							99.0				
4H-6, 74	173.04								1519.3			
5H-2, 110	176.90						143.8	123.0	1538.1			
5H-3, 60	177.90									1.003	0.038	0.0037
5H-4, 90	179.70	47.88	70.18	1.60	0.83	2.59	61.5	103.0	1560.5			
5H-5, 60	180.90									0.906	0.042	0.0030
5H-6, 87	182.67						110.2		1560.5			
5H-7, 60	183.90									1.001	0.031	0.0031
6H-2, 50	185.80									1.111	0.024	0.0036
6H-2, 114	186.44	49.47	73.04	1.64	0.83	2.80	76.5	58.0	1546.8			
6H-3, 50	187.30									0.977	0.018	0.0030
6H-4, 50	188.80									1.023	0.043	0.0028
6H-4, 90	189.20	51.05	75.44	1.54	0.76	2.98	59.1	123.0	1549.0			
6H-6, 50	191.80									0.997	0.038	0.0023
7H-2, 80	195.60						92.8					
7H-2, 100	195.80	48.73	72.01	1.58	0.81	2.73		123.0	1536.8			
7H-4, 66	198.46	49.52	67.28	1.50	0.76	2.11	88.1	89.0	1556.7			
7H-6, 94	201.74	49.07	72.89	1.63	0.83	2.82	74.2	123.0	1603.2			
8H-2, 70	205.00									0.876	0.012	0.0046
8H-2, 97	205.27							145.0	1549.3			
8H-3, 70	206.50									1.016	0.041	0.0027
8H-4, 5	207.35	50.72	69.88	1.48	0.73	2.27	68.4	145.0	1607.0			
9H-2, 40	211.20									0.942	0.037	0.0043
9H-3, 95	213.25	55.80	75.49	1.47	0.65	2.46	37.1	30.0	1595.1			
9H-4, 40	214.20									0.981	0.024	0.0030
9H-6, 40	217.20									1.021	0.045	0.0027
9H-6, 30	217.10	48.34	67.84	1.58	0.82	2.27	92.8	175.0	1574.6			
9H-CC, 5	217.47	50.61	70.78	1.56	0.77	2.38	29.0	58.0	1574.4			
10H-2, 70	220.00									0.993	0.026	0.0033
10H-2, 91	220.21	51.72	72.08	1.50	0.72	2.43	106.7	123.0	1559.7			
10H-4, 70	223.00									0.950	0.026	0.0035
10H-4, 75	223.05	50.61	71.82	1.50	0.74	2.51	105.5	123.0	1569.6			
10H-6, 70	226.00									0.941	0.022	0.0030
10H-6, 74	226.04	54.03	74.99	1.47	0.68	2.57	74.2	175.0	1556.0			
11X-2, 70	229.50	53.92	76.40	1.60	0.74	2.79	60.3	235.0	1561.0			
11X-4, 90	232.70	47.13	70.08	1.66	0.88	2.65	61.5	215.0	1578.4			
11X-7, 15	236.45	51.42	71.80	1.57	0.76	2.42	36.0	145.0	1587.1			
13X-1, 87	243.07								1548.9			
13X-1, 89	243.09	48.27	70.73	1.53	0.79	2.62						
13X-1, 91	246.09						67.3					
13X-3, 70	245.90									0.898	0.020	0.0030
13X-3, 91	246.11	48.85	71.28	1.48	0.76	2.62						
13X-3, 93	246.13							89.0	1549.8			
13X-5, 19	248.39								1539.0			
13X-5, 20	248.40							89.0				
13X-5, 21	248.41	48.74	73.18	1.55	0.79	2.90						
13X-5, 24	248.44						56.8					
13X-5, 70	248.90									1.001	0.047	0.0040
13X-7, 20	251.40									0.901	0.008	0.0027
14X-1, 25	252.05						71.9					
14X-1, 26	252.06	50.29	71.53	1.48	0.74	2.51						
14X-1, 27	252.07							89.0	1527.8			
15X-1, 67	262.17	44.21	65.73	1.57	0.88	2.45		173.0	1579.4			
16X-1, 44	271.54							122.9				
16X-1, 46	271.56	50.71	71.60	1.53	0.76	2.47		165.0	1563.8			

SUMMARY AND CONCLUSIONS

Drilling at Site 746 is a continuation of the program that was begun at Site 745, about 5 km to the south. Drilling at Site 745 had been terminated at 215.0 mbsf after an iceberg approached the site. Site 746 is located above a seismically equivalent section to that beneath Site 745, and seismic stratigraphy indicated that stratigraphic horizons at Site 746 should lie between 19 and 26 m shallower than age-equivalent horizons in Hole 745B. The upper section of Hole 746A above 164.8 mbsf was washed, with the exception of a spot core taken between 106.8 and 116.3 mbsf to check correlation with Hole 745B. Thereafter, Hole 746A was continuously cored down to 280.8 mbsf, the total depth, where upper Miocene diatomaceous sediment was recovered. Site 746 was also terminated because an iceberg approached the drilling location. Biostratigraphy and magnetostratigraphy indicate that stratigraphic horizons in Hole 746A are between 40 and 50 m deeper than equivalent horizons in Hole 745B, a figure which

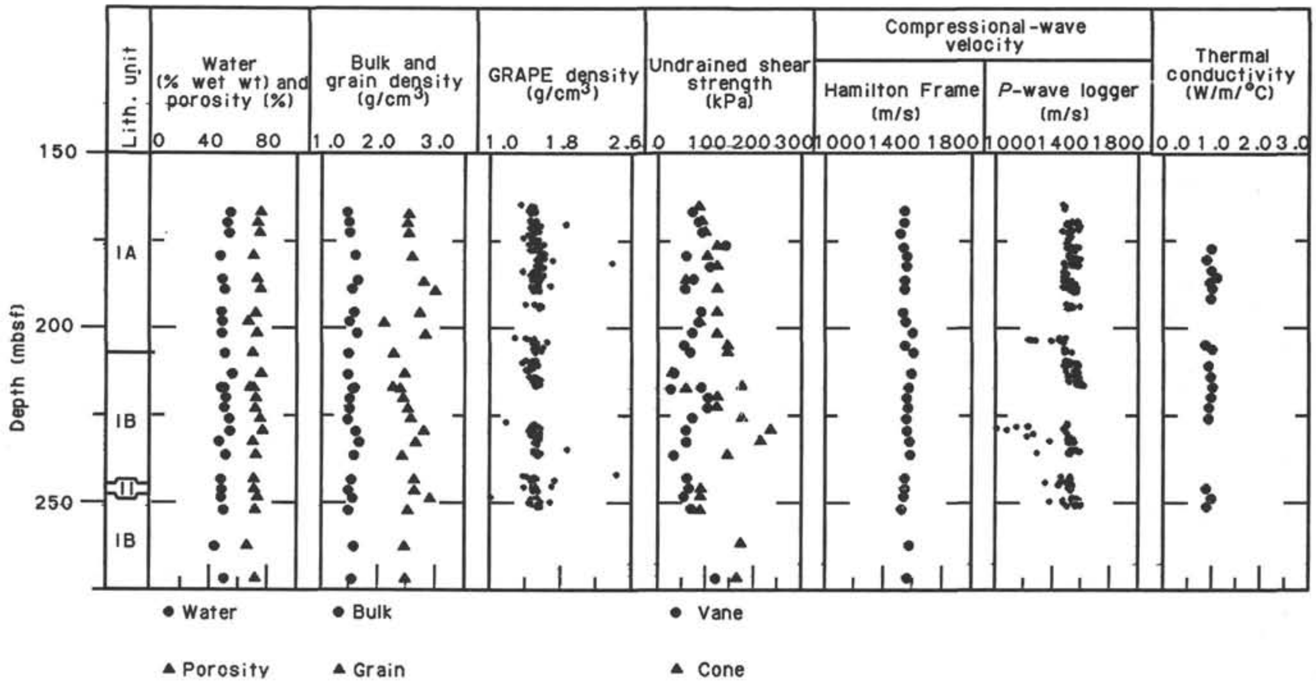

Figure 11. Physical-properties profiles for Site 746. No geotechnical units were distinguished at Site 746.

reflects in part the shallower water depth (4059 vs. 4082 m) of Site 746. Consequently, continuous coring at Site 746 began roughly where coring was terminated at Site 745 (about 5.7 Ma), and Site 746 extended the record at Site 745 by about 116 m.

The lithologic and geotechnical units found at Site 746 closely resemble those at Site 745. The sequence cored at Site 746 consists of mixed biosiliceous and terrigenous sediments and is assigned to one lithologic unit. In the upper part of the recovered section, clayey diatom ooze alternates with diatomaceous clay and silty clay in crude cycles, which are 6 cm to several meters thick. The boundaries between these cycles are mostly gradational, and only a few display sharp contacts. This relationship persists downhole to about 217.8 mbsf, where a gradational change occurs. Here the sediment becomes more lithified, more pervasively bioturbated, and contains less distinct cycles, but is more fractured. This gradational change separates lithologic Subunits IA and IB, and only one other Unit II, a 58-cm-thick nannofossil ooze at 246.7 to 247.3 mbsf, is recognized in Hole 746A.

Coarse grains, granules, and minor small pebbles are uniformly disseminated throughout Subunit IA. These appear to be ice rafted, as most clasts are fresh, subrounded to subangular, and are composed predominantly of quartz. The larger clasts, however, display a wider range of lithologies, including granite, amphibolite, and various types of gneiss. Similar grains and granules are found in Subunit IB, but they are less common.

Sediments recovered from Hole 746A show a continuation of physical-property trends found in the lower part of the drilled sequence at Site 745, and they are considered to belong to geotechnical subunit G2C of that site. Water content and porosity follow a slight linear decrease with depth, while bulk density displays a slight increase. Shear strength, despite a relatively large scatter, seems to become more constant, relative to Site 745 trends, while compressional-wave velocity and thermal conductivity stay essentially constant downhole. As at Site 745, sediments cored at Site 746 are in a state of underconsolidation, probably reflecting a relatively rapid rate of sedimentation.

Table 5. Seismic reflections recorded for Sites 745 and 746 and near Site 746 and seafloor depths for those three locations.

	Depth		
Reflector	Site 745 (mbsf)	Site 746 (mbsf)	Southeast of Site 746 1 km (mbsf)
AA	52	41	
BB	108	82	
CC	147		202 (tracing?)
DD	197		256 (tracing fair)
EE	267		341 (tracing good)

Site	Seafloor[a] (m below sea level)
745	4082
746	4059
746 (1 km southeast)	4191

[a] Actual depths below seafloor may be 1 m deeper than indicated due to a slightly higher sound velocity in sediments.

Diverse, well-preserved diatom assemblages are present in all of the core-catcher samples from Hole 746A. Radiolarians are abundant and well preserved in the upper part of the sequence recovered, but they become less common below 227.3 mbsf. Biosiliceous biostratigraphy indicates that sediment cored at the bottom of Hole 746A is late Miocene in age and younger than 10 Ma. As at Site 745, calcareous microfossils are absent from most of the succession. The nannofossil ooze of Unit II contains a strongly etched, low-diversity assemblage, which is of little use for biostratigraphy.

Magnetostratigraphy identifies a series of reversed and normally polarized intervals that should be correlatable to the geomagnetic polarity time scale after further study onshore and refined biostratigraphic study. Preliminary study indicates that magnetic polarity Chron C5 may be represented below 240 mbsf.

Carbonate is >1% throughout Hole 746A, except in 58-cm-thick lithologic Unit II, where it increases to 4.6%. Sediment recovered from Hole 746A contains low organic carbon, ranging from 0.09% to 0.16%. Bacterial sulfate reduction clearly is taking place at depths greater than 248 mbsf, but low ammonium and phosphate concentrations indicate that the amount of organic matter being consumed at that depth is very small.

As at Site 745, the sediments recovered at Site 746 most likely record glacial-interglacial fluctuations in the sedimentation of biogenic and detrital components. The randomly dispersed coarse sand grains and gravel present in the sediment were probably dropped by icebergs floating over the site. The composition of some of the clasts clearly points to Antarctic basement as the source area, although some glacial input from Kerguelen Island cannot be ruled out. A broad channel separating the sediment ridge containing Sites 745 and 746 from the southern Kerguelen Plateau most likely prevented the deposition at those sites of detrital material transported along the bottom off the southern Kerguelen Plateau. However, transport in suspension is possible. Whether this depression persists to the north is unclear, and transport of detrital material off the more elevated northern portion of Kerguelen Plateau is a possibility. In fact, the occurrence of reworked diatoms and radiolarians of various ages throughout Hole 746A and the presence of benthic diatoms that lived within the photic zone (above 100 m) support this area as a source of some of the transported sediment.

Another important source for detrital material might also have been the Antarctic shelf, because Antarctic Bottom Water originating on the Antarctic slope could transport sediment supplied by the melting of ice sheets grounded at the shelf break during the time of maximum glaciation (see "Summary and Conclusions" section, "Site 745" chapter). Whatever the source of bottom current-transported detrital material, a larger volume of that material was probably transported during glacial times, when both Antarctic Bottom Water flow was increased and currents sweeping over the Kerguelen Plateau were probably stronger because of the shallower water. Consequently, increased detrital sediment input at Sites 745 and 746 during glacial times seems probable as a result of increased ice rafting and/or increased bottom current transport.

REFERENCES

Berggren, W. A., Kent, D. V., Flynn, J. J., and Van Couvering, J. A., 1985. Cenozoic geochronology. *Geol. Soc. Am. Bull.*, 96:1407–1418.

Srivastava, S. P., Arthur, M. A., et al., 1985. *Proc. ODP, Init. Repts.*, 105: College Station, TX (Ocean Drilling Program).

Stumm, W., and Morgan, J. J., 1981. *Aquatic Chemistry*: New York (Wiley).

Zimmerman, H. B., Shackleton, N. J., Backman, J., Kent, D. V., Baldauf, J. G., Kaltenback, A. J., and Morton, A. C., 1985. History of Plio-Pleistocene climate in the northeastern Atlantic, Deep Sea Drilling Project, Hole 552A. *In* Roberts, D. G., Schnitker, D., et al., *Init. Repts. DSDP*, 81: Washington (U.S. Govt. Printing Office), 861–875.

Ms 119A-114

APPENDIX
Leg 119 Sea-Surface Temperature

Date (1987–1988)	Time (UTC)	Latitude (°S)	Longitude (°E)	Temperature (°C)
Dec. 18	1800	20.70	57.20	27.1
19	0000	21.90	57.60	26.5
	0600	22.90	57.80	27.5
	1200	24.00	58.00	27.0
	1800	25.20	58.30	26.8

Appendix (Continued).

Date (1987–1988)	Time (UTC)	Latitude (°S)	Longitude (°E)	Temperature (°C)
20	0000	26.50	58.70	25.8
	0600	27.50	58.90	25.0
	1200	28.70	59.20	24.8
	1800	29.80	59.70	22.0
21	0000	31.00	60.20	22.1
	0600	31.80	60.50	21.9
	1200	33.00	61.20	21.8
	1800	34.00	61.70	21.5
22	0000	35.30	62.40	19.6
	0600	36.30	63.00	18.1
	1200	37.20	63.40	17.8
	1800	38.10	63.90	Missing
23	0000	39.20	64.40	17.8
	0600	40.00	64.90	15.4
	1200	40.90	65.40	13.7
	1800	41.90	66.00	11.9
24	0000	42.80	66.60	12.2
	0600	43.80	67.30	12.3
	1200	44.70	68.00	9.5
	1800	45.90	68.90	7.0
25	0000	47.00	70.00	6.2
	0600	47.60	70.90	5.5
	1200	48.50	71.60	3.8
	1800	49.20	71.50	3.4
	Site 736 (49.40°S, 71.60°E)			
26	0000			3.5
	0600			3.5
	1200			3.5
	1800			3.5
27	0000			3.0
	0600			3.5
	1200			3.5
	1800			3.4
28	0000			3.4
	0600			3.5
	1200			3.7
	1800			3.7
29	0000			3.3
	0600			3.5
	1200			4.0
	1800	49.70	72.20	3.5
30	0000	50.20	73.10	3.4
	Site 737 (50.23°S, 73.03°E)			
	0600			3.5
	1200			3.5
	1800			3.5
31	0000			3.5
	0600			3.4
	1200			3.4
	1800			3.2
Jan. 1	0000			3.9
	0600			3.1
	1200			3.5
	1800			3.5
2	0000			3.1
	0600			3.0
	1200			3.5
	1800			3.3
3	0000			3.0
	0600			3.0
	1200			3.5
	1800			3.5
4	0000			3.2
	0600			3.3
	0705	50.19	73.03	3.5
	0809	50.31	73.03	3.9
	0920	50.46	73.08	3.9
	1050	50.67	73.15	4.0
	1200	50.80	73.20	4.0
	1230	51.08	73.32	4.0
	1608	51.73	73.57	3.5
	1645	51.85	73.62	3.4
	1800	51.90	73.60	3.5
	2050	52.70	74.06	3.4
	2150	52.88	74.19	3.0

Appendix (Continued).

Date (1987–1988)	Time (UTC)	Latitude (°S)	Longitude (°E)	Temperature (°C)
	2232	53.02	74.29	2.9
	2325	53.15	74.43	2.9
5	0000	53.20	74.50	2.9
	0107	53.47	74.62	2.9
	0200	53.63	74.74	2.6
	0215	53.68	74.77	2.6
	0229	53.72	74.81	2.6
	0300	53.82	74.90	2.5
	0340	53.95	74.97	2.5
	0409	54.03	75.05	2.5
	0505	54.21	75.19	2.5
	0538	54.31	75.26	2.5
	0600	54.34	75.13	2.5
	0725	54.65	75.52	2.4
	0828	54.83	75.67	2.4
	1200	55.40	76.10	2.5
	1800	56.40	76.90	1.0
	2122	57.07	77.52	0.9
6	0000	57.60	77.80	0.5
	0045	57.72	77.97	0.5
	0310	58.02	78.34	0.6
	0600	58.50	78.70	0.6
	1200	59.40	79.50	1.0
	1800	60.30	80.50	0.6
7	0000	61.50	80.50	0.4
	0600	62.70	80.50	0.2
	1200	63.70	80.50	0.5
	1800	64.70	79.40	0.3
8	0000	65.80	77.30	−0.7
	0600	66.70	76.10	+0.1
	1200	67.10	75.30	0.1
	1800	66.80	75.50	0.0
9	0000	66.00	77.30	0.2
	0600	65.20	78.60	0.2
	1200	64.30	80.10	0.8
	1800	63.40	81.70	0.8
	Site 738 (62.70°S, 82.80°E)			
10	0000			0.8
	0600			0.8
	1800			1.1
13	0000			0.9
	0600			0.9
	1200			1.1
	1800			0.9
14	0000			1.0
	0600			1.0
	1200			1.0
	1800			1.0
15	0000			0.9
	0600			0.9
	1200			1.0
	1800			1.0
16	0000			0.6
	0600			1.0
	1200			1.0
	1800			1.0
17	0000			1.2
	0600	63.40	81.60	1.1
	1200	64.10	80.50	1.4
	1800	65.00	78.90	0.7
18	0000	66.20	76.90	0.5
	0600	67.20	75.20	0.2
	Site 739 (67.30°S, 75.10°E)			
	1200			0.5
	1800			0.2
19	0000			0.0
	0600			0.0
	1200			0.1
	1800			0.0
20	0000			0.4
	0600			−0.1
	1200			+0.4
	1800			0.6
21	0000			0.2
	0600			0.2

Appendix (Continued).

Date (1987–1988)	Time (UTC)	Latitude (°S)	Longitude (°E)	Temperature (°C)
	1200			0.7
	1800			0.9
22	0000			0.2
	0600			0.4
	1200			0.4
	1800			0.7
23	0000			0.4
	0600	68.10	75.90	1.2
	1200	68.70	76.80	3.2
	Site 740 (68.70°S, 76.80°E)			
	1800			1.3
24	0000			0.5
	0600			0.8
	1200			1.0
	1800			1.5
25	0000			0.4
	0600			0.4
	1200			1.6
	1800			1.0
26	0000			0.1
	0600			0.2
	1200			1.0
	1800			Missing
27	0000			1.1
	0600			0.6
	1200			1.9
	1800	68.40	76.40	1.7
	Site 741 (68.40°S, 76.30°E)			
28	0000			0.8
	0600			1.5
	1200			1.7
	1800			1.6
29	0000			1.4
	0600			0.9
	1200	68.10	76.10	1.3
	1800	67.60	75.50	1.1
	Site 742 (67.50°S, 75.40°E)			
30	0000			0.8
	0600			0.8
	1200			1.0
	1800			1.0
31	0000			0.8
	0600			0.8
	1200			0.7
	1800			0.7
Feb. 1	0000			0.8
	0600			0.8
	1200			0.7
	1800			0.7
2	0000			0.8
	0600	67.30	75.10	0.6
	1200	66.90	74.60	0.8
	Site 743 (69.90°S, 74.70°E)			
	1800			0.7
3	0000			0.8
	0600			0.8
	1200			0.8
	1800	66.70	76.80	1.0
4	0000	65.80	76.80	0.8
	0600	65.10	78.30	1.2
	1200	64.40	79.50	1.5
	1800	63.70	81.10	1.5
5	0000	62.90	82.30	1.5
	0600	62.30	82.20	1.5
	1200	61.70	81.20	1.5
	Site 744 (61.60°S, 80.60°E)			
	1800			1.2
6	0000			1.2
	0600			1.2

Appendix (Continued).

Date (1987–1988)	Time (UTC)	Latitude (°S)	Longitude (°E)	Temperature (°C)
	1200			1.5
	1800			1.2
7	0000			1.5
	0600			1.6
	1200	61.50	80.60	1.4
	1800	60.90	82.30	2.0
	2210	60.57	83.17	1.9
8	0000	60.40	83.70	2.0
	0311	59.98	84.73	1.6
	0600	59.80	85.20	1.5
	1200	59.50	85.90	2.0
	Site 745 (59.60°S, 85.90°E)			
	1800			1.6
9	0000			1.5
	0600			1.6
	1200			1.8
	1800			1.6
10	0000			1.6
	0600			1.8
	1200			2.0
	Site 746 (59.50°S, 85.90°E)			
	1800			2.0
11	0000			1.6
	0600			1.8
	1200			1.8
	1800			1.8
12	0000			1.6
	0600			1.7
	1200			1.8
	1800			1.8

Appendix (Continued).

Date (1987–1988)	Time (UTC)	Latitude (°S)	Longitude (°E)	Temperature (°C)
	2010	59.49	86.09	2.6
	2104	59.42	86.13	2.7
	2202	59.33	86.15	2.6
13	0000	59.10	86.53	2.7
	0155	58.73	86.97	2.9
	0400	58.42	87.43	3.0
	0600	58.10	87.90	3.5
	0756	57.79	88.31	3.5
	0950	57.51	88.66	3.0
	1120	57.34	88.88	3.5
	1200	57.25	89.00	3.4
	1600	56.60	89.90	3.8
	1830	56.21	90.42	3.4
	2110	55.81	90.93	2.6
	2155	55.70	91.10	2.9
	2259	55.54	91.31	3.0
14	0000	55.30	91.56	3.2
	0305	54.87	92.15	3.2
	0400	54.73	92.33	3.0
	0600	54.40	92.80	3.4
	0826	53.98	93.28	4.3
	0935	53.79	93.48	4.9
	1031	53.65	93.66	4.7
	1143	53.44	93.87	4.5
	1445	52.95	94.43	4.7
	1630	52.70	94.70	4.5
	2115	52.04	95.63	6.8
	2225	51.86	95.86	6.8
15	0000	51.60	96.10	6.8
	0225	51.29	96.46	6.1
	0500	50.92	96.85	6.0
	0600	50.80	97.00	6.1